# MODIS ATMOSPHERIC PROFILE RETRIEVAL ALGORITHM THEORETICAL BASIS DOCUMENT

SUZANNE W. SEEMANN[1], EVA E. BORBAS[1], JUN LI[1], W. PAUL MENZEL[2], LIAM E. GUMLEY[1]

*Cooperative Institute for Meteorological Satellite Studies*

*University of Wisconsin-Madison*

*1225 W. Dayton St.*

*Madison, WI 53706*

Version 6

October 25, 2006

---

1 CIMSS (Suzanne.Seemann@ssec.wisc.edu)

2 NOAA/NESDIS (Paul.Menzel@ssec.wisc.edu)

TABLE OF CONTENTS

## 1. *Introduction*

The purpose of this document is to present an algorithm for retrieving vertical profiles of atmospheric temperature and moisture from multi-wavelength thermal radiation measurements in clear skies. While the MODIS is not a sounding instrument, it does have many of the spectral bands found on the High resolution Infrared Radiation Sounder (HIRS) currently in service on the polar orbiting NOAA TIROS Operational Vertical Sounder (TOVS). Thus it is possible to generate profiles of temperature and moisture as well as total column estimates of precipitable water vapor, ozone, and atmospheric stability from the MODIS infrared radiance measurements. These parameters can be used to correct for atmospheric effects for some of the MODIS products (such as sea surface and land surface temperatures, ocean aerosol properties, water leaving radiances, photosynthetically active radiation) as well as to characterize the atmospheric state for global greenhouse studies. The MODIS algorithms were adapted from the operational HIRS and GOES algorithms, with adjustments to accommodate the absence of stratospheric sounding spectral bands and to realize the advantage of greatly increased spatial resolution (1 km MODIS versus 17 km HIRS) with good radiometric signal to noise (better than 0.35 C for typical scene temperatures in all spectral bands).

In this document, we offer some background to the retrieval problem, review the MODIS instrument characteristics, describe the theoretical basis of the MODIS retrieval algorithm, discuss the practical aspects of the algorithm implementation, and provide some validation of products.

## 2. *Overview and background information*

This paper details the operational MODIS MOD07_L2 algorithm for retrieving vertical profiles (soundings) of temperature and moisture, total column ozone burden, integrated total column precipitable water vapor, and several atmospheric stability indices (Seemann et al. 2003, Seemann et al. 2006). The MODIS atmospheric profile algorithm is a statistical regression with the option for a subsequent non-linear physical retrieval. The retrievals are performed using clear sky radiances measured by MODIS within a 5x5 field of view (approximately 5km resolution) over land and ocean for both day and night. A version of the algorithm using only the statistical

regression is operational at the Goddard Distributed Active Archive Center (GDAAC) processing system (http://daac.gsfc.nasa.gov/MODIS).

The retrieval methods presented here are based on the work of Li (2000), and work by Smith and Woolf (1988) and Hayden (1988). The clear advantage of MODIS for retrieving atmospheric profiles is its combination of fifteen infrared spectral channels suitable for sounding and high spatial resolution suitable for imaging (1 km at nadir). Temperature and moisture profiles at MODIS spatial resolution are required by a number of other MODIS investigators, including those developing sea surface temperature and land surface temperature retrieval algorithms. Total ozone and precipitable water vapor estimates at MODIS resolution are required by MODIS investigators developing atmospheric correction algorithms. The combination of high spatial resolution sounding data from MODIS, and high spectral resolution sounding data from AIRS, will provide a wealth of new information on atmospheric structure in clear skies.

## 2.1 *History*

Inference of atmospheric temperature profiles from satellite observations of thermal infrared emission was first suggested by King (1956). In this pioneering paper, King pointed out that the angular radiance (intensity) distribution is the Laplace transform of the Planck intensity distribution as a function of the optical depth, and illustrated the feasibility of deriving the temperature profile from the satellite intensity scan measurements. Kaplan (1959) advanced the temperature sounding concept by demonstrating that vertical resolution of the temperature field could be inferred from the spectral distribution of atmospheric emission. Kaplan noted that observations in the wings of a spectral band sense deeper regions of the atmosphere, whereas observations in the band center see only the very top layer of the atmosphere, since the radiation mean free path is small. Thus by properly selecting a set of sounding spectral channels at different wavelengths, the observed radiances could be used to make an interpretation of the vertical temperature distribution in the atmosphere.

Wark (1961) proposed a satellite vertical sounding program to measure atmospheric temperature profiles, and the first satellite sounding instrument (SIRS-A) was launched on NIMBUS-3 in 1969 (Wark and Hilleary, 1970). Successive experimental instruments on the NIMBUS series of polar orbiting satellites led to the development of the TIROS-N series of

operational polar-orbiting satellites in 1978. These satellites introduced the TIROS Operational Vertical Sounder (TOVS, Smith et al. 1979), consisting of the High-resolution Infrared Radiation Sounder (HIRS), the Microwave Sounding Unit (MSU), and the Stratospheric Sounding Unit (SSU). This same series of instruments continues to fly today on the NOAA operational polar orbiting satellites. HIRS provides 17 km spatial resolution at nadir with 19 infrared sounding channels. The first sounding instrument in geostationary orbit was the GOES VISSR Atmospheric Sounder (VAS, Smith et al. 1981) launched in 1980. The current generation GOES-8 sounder (Menzel and Purdom, 1994) provides 8 km spatial resolution with 18 infrared sounding channels; the GOES retrieval algorithm is detailed in Ma et al. (1999). An excellent review of the history of satellite temperature and moisture profiling is provided by Smith (1991).

## 2.2 *Instrument Characteristics*

MODIS is a scanning spectroradiometer with 36 spectral bands between 0.645 and 14.235 μm (King et al. 1992). Table 1 summarizes the MODIS technical specifications.

**Table 1**: MODIS Technical Specifications

| | |
|---|---|
| Orbit: | 705 km altitude, sun-synchronous, 10:30 a.m. descending node |
| Scan Rate: | 20.3 rpm, cross track |
| Swath Dimensions: | 2330 km (cross track) by 10 km (along track at nadir) |
| Quantization: | 12 bits |
| Spatial Resolution: | 250 m (bands 1-2), 500 m (bands 3-7), 1000 m (bands 8-36) |

Table 2 shows the MODIS spectral bands that are used in the MODIS algorithm. Note that in most cases the predicted (goal) noise is expected to better than the specification. The data rate with 12 bit digitization and a 100% duty cycle is expected to be approximately $5.1\times10^6$ bits/sec (55 Gbytes/day). Although each band is assigned a "Primary Atmospheric Application," all 11 bands are included in the calculation of the regression retrieval coefficients that are in turn used to derive the products.

**Table 2**: MODIS Spectral Band Specifications

| Primary Atmospheric Application | Band | Bandwidth[1] | $T_{typical}$ (K) | Radiance[2] at $T_{typical}$ | NEΔT (K) Specification | NEΔT (K) Predicted |
|---|---|---|---|---|---|---|
| Temperature profile | 25 | 4.482-4.549 | 275 | 0.59 | 0.25 | 0.10 |
| Moisture profile | 27 | 6.535-6.895 | 240 | 1.16 | 0.25 | 0.05 |
| | 28 | 7.175-7.475 | 250 | 2.18 | 0.25 | 0.05 |
| | 29 | 8.400-8.700 | 300 | 9.58 | 0.05 | 0.05 |
| Ozone | 30 | 9.580-9.880 | 250 | 3.69 | 0.25 | 0.05 |
| Surface Temperature | 31 | 10.780-11.280 | 300 | 9.55 | 0.05 | 0.05 |
| | 32 | 11.770-12.270 | 300 | 8.94 | 0.05 | 0.05 |
| Temperature profile | 33 | 13.185-13.485 | 260 | 4.52 | 0.25 | 0.15 |
| | 34 | 13.485-13.785 | 250 | 3.76 | 0.25 | 0.20 |
| | 35 | 13.785-14.085 | 240 | 3.11 | 0.25 | 0.25 |
| | 36 | 14.085-14.385 | 220 | 2.08 | 0.35 | 0.35 |

[1] μm at 50% response

[2] W $m^{-2}$ $sr^{-1}$ $\mu m^{-1}$

Figure 1 shows the spectral responses of the MODIS infrared bands in relation to an atmospheric emission spectrum computed by a line-by-line radiative transfer model (LBL-RTM) for the US standard atmosphere.

**Figure 1**: MODIS infrared spectral response. Nadir viewing emission spectrum of U.S. Standard Atmosphere from LBL-RTM.

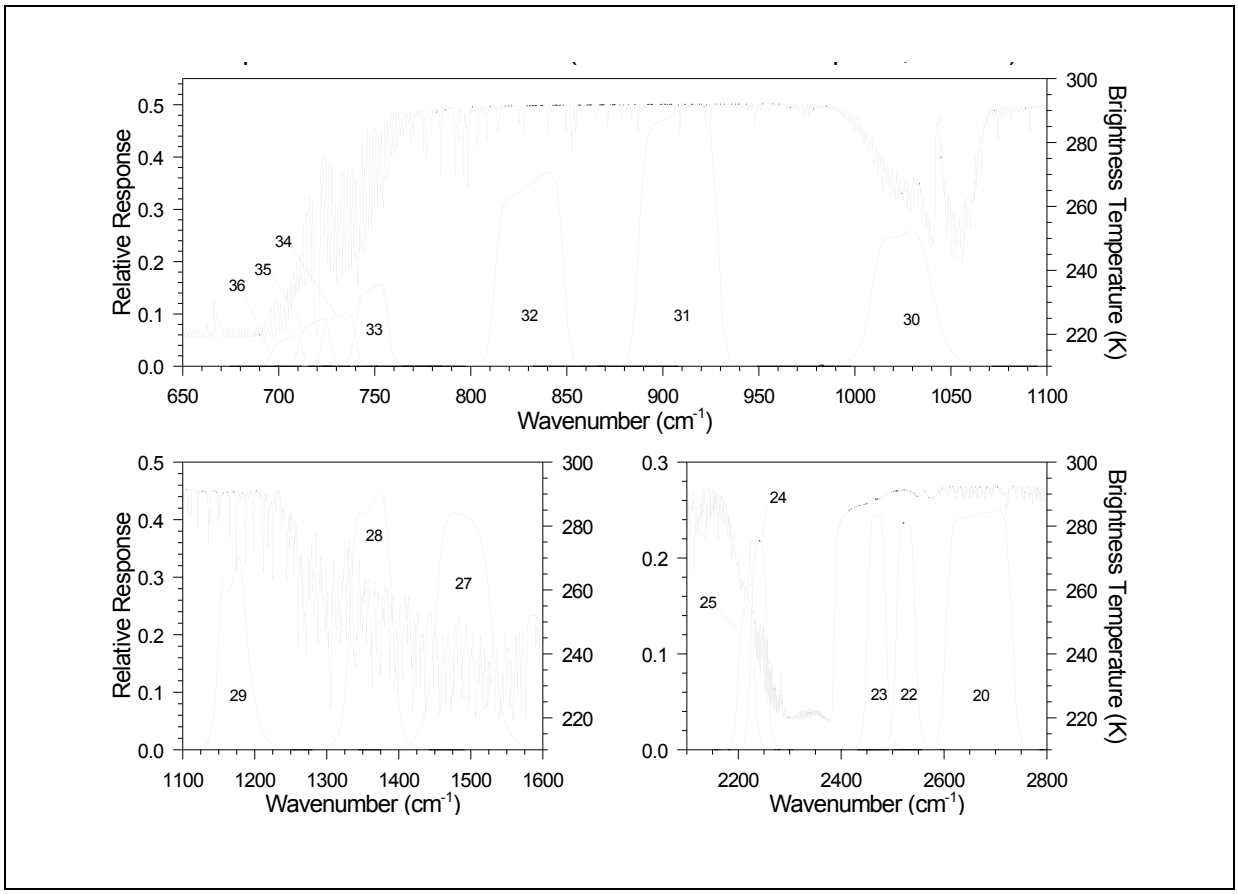

## 3. *Algorithm Description*

In section we describe the theoretical basis and practical implementation of the atmospheric profile retrieval algorithm.

### 3.1 *Theoretical Background*

In order for atmospheric temperature to be inferred from measurements of thermal emission, the source of emission must be a relatively abundant gas of known and uniform distribution. Otherwise, the uncertainty in the abundance of the gas will make ambiguous the determination of temperature from the measurements. There are two gases in the earth-atmosphere that are present in uniform abundance for altitudes below about 100 km, and show emission bands in the spectral regions that are convenient for measurement. Carbon dioxide, a minor constituent with a relative volume abundance of 0.003, has infrared vibrational-rotational bands. Oxygen, a major constituent with a relative volume abundance of 0.21, also satisfies the requirement of a uniform mixing ratio and has a microwave spin-rotational band. In addition, the emissivity of the earth surface in the surface sensitive spectral bands must be characterized and accounted for.

There is no unique solution for the detailed vertical profile of temperature or an absorbing constituent because (a) the outgoing radiances arise from relatively deep layers of the atmosphere, (b) the radiances observed within various spectral channels come from overlapping layers of the atmosphere and are not vertically independent of each other, and (c) measurements of outgoing radiance possess errors. As a consequence, there are a large number of analytical approaches to the profile retrieval problem. The approaches differ both in the procedure for solving the set of spectrally independent radiative transfer equations (e.g., matrix inversion, numerical iteration) and in the type of ancillary data used to constrain the solution to insure a meteorologically meaningful result (e.g., the use of atmospheric covariance statistics as opposed to the use of an a priori estimate of the profile structure). There are some excellent papers in the literature which review the retrieval theory which has been developed over the past few decades (Fleming and Smith, 1971; Fritz et al., 1972; Rodgers, 1976; Twomey, 1977; and Houghton et al. 1984). The following sections present the mathematical basis for two of the procedures which

have been utilized in the operational retrieval of atmospheric profiles from satellite measurements.

### 3.2 *Statistical Regression Profile Retrieval*

A computationally efficient method for determining temperature and moisture profiles from satellite sounding measurements uses previously determined statistical relationships between observed (or modeled) radiances and the corresponding atmospheric profiles. This method is often used to generate a first-guess for a physical retrieval algorithm, as is done in the International TOVS Processing Package (ITPP, Smith et al., 1993). The statistical regression algorithm for atmospheric temperature is described in detail in Smith et. al. (1970), and can be summarized as follows (the algorithm for moisture profiles is formulated similarly). In cloud-free skies, the radiation received at the top of the atmosphere at frequency ν is the sum of the radiance contributions from the Earth's surface and from all levels in the atmosphere,

$$R(\nu_j) = \sum_{i=1}^{N} B[\nu_j, T(p_i)] w(\nu_j, p_i) \qquad (1)$$

where

$w(\nu_j, p_i) = \varepsilon(\nu_j, p_i) \tau(\nu_j, 0 \rightarrow p_i)$ is the weighting function,

$B[\nu_j, T(p_i)]$ is the Planck radiance for pressure level $i$ at temperature $T$,

$\varepsilon(\nu_j, p_i)$ is the spectral emissivity of the emitting medium at pressure level $i$,

$\tau(\nu_j, 0 \rightarrow p_i)$ is the spectral transmittance of the atmosphere above pressure level $i$.

The problem is to determine the temperature (and moisture) at $N$ levels in the atmosphere from $M$ radiance observations. However because the weighting functions are broad and represent an average radiance contribution from a layer, the $M$ radiance observations are interdependent, and hence there is no unique solution. Furthermore, the solution is unstable in that small errors in the radiance observations produce large errors in the temperature profile. For this reason, the solution is approximated in a linearized form. First (1) is re-written in terms of a deviation from an initial state,

$$R(\nu_j) - R_0(\nu_j) = \sum_{i=1}^{N} \{B[\nu_j, T(p_i)] - B[\nu_j, T_0(p_i)]\} w(\nu_j, p_i) + e(\nu_j) \qquad (2)$$

where

$e(\nu_j)$ is the measurement error for the radiance observation.

In order to solve (2) for the temperature profile $T$ it is necessary to linearize the Planck function dependence on frequency. This can be achieved since in the infrared region the Planck function is much more dependent on temperature than frequency. Thus the general inverse solution of (2) for the temperature profile can be written as

$$T(p_i) - T_0(p_i) = \sum_{j=1}^{M} A(\nu_j, p_i)\left[R(\nu_j) - R_0(\nu_j)\right] \tag{3}$$

or in matrix form

$$T = AR$$

where $A(\nu_j, p_i)$ is a linear operator. Referring back to (2), it can be seen that in theory $A$ is simply the inverse of the weighting function matrix. However in practice the inverse is numerically unstable.

The statistical regression algorithm seeks a "best-fit" operator matrix $A$ that is computed using least squares methods by utilizing a large sample of atmospheric temperature and moisture soundings, and collocated radiance observations. That is, we seek to minimize the error

$$\frac{\partial}{\partial A}\left|AR - T\right|^2 = 0$$

which is solved by the normal equations to yield

$$A = \left(R^T R\right)^{-1} R^T T \tag{5}$$

where

$\left(R^T R\right)$ is the covariance of the radiance observations,

$\left(R^T T\right)$ is the covariance of the radiance observations with the temperature profile.

Ideally, the radiance observations would be taken from actual MODIS measurements and used with time and space co-located radiosonde profiles to directly derive the regression coefficients $A$. In such an approach, the regression relationship would not involve any radiative transfer calculations. However, radiosondes are routinely launched only two times each day at 0000 UTC and 1200 UTC simultaneously around the earth; Terra passes occur at roughly 1100-

1200 AM and 1000-1100 PM local standard time each day. It is therefore not possible to obtain many time and space co-located MODIS radiances. Alternatively, the regression coefficients can also be generated from MODIS radiances calculated using a transmittance model with profile input from a global temperature and moisture radiosonde database. In this approach, the accuracy of the atmospheric transmittance functions for the various spectral bands is crucial for accurate parameter retrieval.

In the regression procedure, the primary predictors are MODIS infrared spectral band brightness temperatures. The algorithm uses 11 infrared bands with wavelengths between 4.5μm and 14.2μm. The retrieval algorithm requires calibrated, navigated, coregistered 1 km FOV radiances from bands 25 (4.52 μm shortwave CO2 absorption band), 27-29 (6.72 to 8.55 μm for moisture information), 30 (9.73 μm for ozone), 31-32 (11.03 and 12.02 split window), and 33-36 (13.34, 13.64, 13.94, and 14.24 μm CO2 absorption band channels). Estimates of surface pressure, latitude, percent land, and month are also used as predictors to improve the retrieval. Table 3 lists the predictors and their noise used in the regression procedure. Quadratic terms of all brightness temperatures in Table 3 are also used as predictors to account for the moisture non-linearity in the MODIS radiances. The noise used in the algorithm is larger than estimates of post-launch detector noise in order to account for variability between the ten detectors (striping). The regression coefficients are generated for 680 local zenith angles from nadir to 65$^{o}$.

**Table 3**: Predictors and their uncertainty used in the regression procedure

| Predictor | Noise used in MOD07 algorithm | Post-launch NEdT averaged over detectors |
|---|---|---|
| Band 25 BT (4.52μm) | 0.75 $^{o}$K | 0.086 $^{o}$K (band 25) |
| Band 27 BT (6.7μm) | 0.75$^{o}$K | 0.376 $^{o}$K |
| Band 28 BT (7.3μm) | 0.75$^{o}$K | 0.193 $^{o}$K |
| Band 29 BT (8.55μm) | 0.189$^{o}$K | 0.189 $^{o}$K |
| Band 30 BT (9.73μm) | 0.75$^{o}$K | 0.241 $^{o}$K |
| Band 31 BT (11μm) | 0.167$^{o}$K | 0.167 $^{o}$K |

| | | |
|---|---|---|
| Band 32 BT (12μm) | 0.192°K | 0.192 °K |
| Band 33 BT (13.3μm) | 0.75°K | 0.308 °K |
| Band 34 BT (13.6μm) | 0.75°K | 0.379 °K |
| Band 35 BT (13.9μm) | 0.75°K | 0.366 °K |
| Band 36 BT (14.2μm) | 1.05°K | 0.586 °K |
| Surface Pressure | 5 hPa | -- |
| Latitude | 0.0 | -- |
| Month | 0.0 | -- |
| Percent Land | 0.0 | -- |

The regression coefficients are generated using the calculated synthetic radiances and the matching atmospheric profile. To perform the regression, Eq.(5) can be applied to the actual MODIS measurements to obtain the estimated atmospheric profiles; integration yields the total precipitable water or total column ozone. The advantage of this approach is that it does not need MODIS radiances collocated in time and space with atmospheric profile data, it requires only historical profile observations. However, it involves the radiative transfer calculations and requires an accurate forward model in order to obtain a reliable regression relationship. Any uncertainties (e.g., a bias of the forward model) in the radiative calculations will influence the retrieval. To address model uncertainties, radiance bias adjustments have been implemented in the retrieval algorithm as discussed in section 4.2. Calculations of the synthetic MODIS radiances require a physically realistic characterization of the surface, including land surface emissivity, skin temperature and surface pressure. These parameters are discussed in section 4.4.

### 3.3 *Physical Profile Retrieval*

The statistical regression algorithm has the advantage of computational efficiency, numerical stability, and simplicity. However, it does not account for the physical properties of the radiative transfer equation (RTE). After computing atmospheric profiles from the regression technique, a

non-linear iterative physical algorithm (Li et al., 2000) applied to the RTE often improves the solution. The physical retrieval approach is described in this section, however it is not currently employed in the operational algorithm due to constraints on computation time.

The physical procedure is based on the regularization method (Li et al., 2000) by minimizing the penalty function defined by

$$Y(X) = \left\| Y^m - Y(X) \right\|^2 + \gamma \left\| X - X_0 \right\|^2 \qquad (6)$$

to measure the degree of fit of the MODIS spectral band measurements to the regression first guess. In equation 6, $X$ is the atmospheric profile to be retrieved, $X_0$ is the initial state of the atmospheric profile or the first guess from regression, $Y^m$ is the vector of the observed MODIS brightness temperatures used in the retrieval process, $Y(X)$ is the vector of calculated MODIS brightness temperatures from an atmospheic state ($X$), and $\gamma$ is the regularization parameter that can be determined by the Discrepancy Principle (Li and Haung, 1999; Li et al. 2000). The solution provides a balance between MODIS spectral band radiances and the first guess. If a radiative transfer calculation using the first guess profile as input fits all the MODIS spectral band radiances well, less weight is given to the MODIS measurements in the non-linear iteration, and the solution will be only a slight modification of the first guess. However, if the first guess does not agree well with the MODIS spectral band radiances, then the iterative physically retrieved profile will be given a larger weight. Thus, the temperature, moisture, and ozone profiles as well as the surface skin temperature will be modified in order to obtain the best simultaneous fit to all the MODIS spectral bands used. For more details, see Li et al. (2000).

### 3.4 *Derived Products*

#### 3.4.1 *Total column precipitable water vapor and ozone*

Determination of the total column precipitable water vapor and total ozone is performed by integrating moisture and ozone profiles through the atmospheric column. The total column

precipitable water vapor "Water_Vapor" parameter included in the MODIS MOD07_L2 data is integrated from the 101-level retrieved mixing ratio profiles. Atmospheric profile retrievals are saved at only 20 levels in the MOD07 data so integration by the user of the 20-level profiles may not result in the same value reported in the "Water_Vapor" field. Another total column water vapor parameter, "Water_Vapor_Direct" is obtained by direct regression from the integrated moisture in the training data.

### 3.4.2 *Atmospheric Stability*

One measure of the thermodynamic stability of the atmosphere is the total-totals index, defined by

$$TT = T_{850} + TD_{850} - 2\,T_{500}$$

where $T_{850}$ and $T_{500}$ are the temperatures at the 850 mb and 500 mb levels, respectively, and $TD_{850}$ is the 850-mb level dew point. *TT* is traditionally estimated from radiosonde point values. For a warm moist atmosphere underlying cold mid-tropospheric air, *TT* is high (e.g., 50-60 K) and intense convection can be expected. There are two limitations of radiosonde derived *TT*: (a) the spacing of the data is too large to isolate local regions of probable convection and (b) the data are not timely since they are available only twice per day.

If we define the dew point depression at 850 mb, $D_{850} = T_{850} - TD_{850}$ , then

$$TT = 2\left(T_{850} - T_{500}\right) - D_{850}$$

Although point values of temperature and dew point cannot be observed by satellite, the layer quantities observed can be used to estimate the temperature lapse rate of the lower troposphere ($T_{850}$ - $T_{500}$) and the low level relative moisture concentration $D_{850}$. Assuming a constant lapse rate of temperature between the 850 and 200 mb pressure levels and also assuming that the dew point depression is proportional to the logarithm of relative humidity, it can be shown from the hydrostatic equation that

$$TT = 0.1489DZ_{850-500} - 0.0546DZ_{850-200} + 16.03\ln(RH)$$

where *DZ* is the geopotential thickness in meters and *RH* is the lower tropospheric relative humidity, both estimated from the MODIS radiance measurements.

Smith and Zhou (1982) reported several case studies using this approach. They found general agreement in gradients in space and time, with the satellite data providing much more spatial detail than the sparse radiosonde observations.

Another estimate of atmospheric stability is the lifted index, which can be derived from the MODIS determined temperature and moisture profile. The lifted index is the difference of the measured 500 mb temperature and the temperature calculated by lifting a surface parcel dry adiabatically to its local condensation level and then moist adiabatically to 500 mb. As this value goes negative it indicates increased atmospheric instability.

## 4.0 *Operational Retrieval Implementation*

The operational MODIS retrieval algorithm consists of several procedures that include cloud detection, averaging clear radiances from 5 by 5 field-of-view (FOV) areas, bias adjustment of MODIS brightness temperatures for forward model and instrument, regression retrieval, and an option to perform a physical retrieval. Because of computer limitations, the MODIS MOD07_L2 retrieval algorithm that is operational at GDAAC processing system includes only the regression retrieval. A version of the algorithm with the physical retrieval will be available for MODIS direct broadcast processing as part of the International MODIS/AIRS Processing Package (IMAPP, Huang et al., 2004) developed at the Space Science and Engineering Center (SSEC) at the University of Wisconsin-Madison (http://cimss.ssec.wisc.edu/~gumley/IMAPP/IMAPP.html). The radiative transfer calculation of the MODIS spectral band radiances is performed using a transmittance model called Pressure layer prototype-Community Radiative Transfer Model (prototype-CRTM, Kleespies et al. 2004); this model uses an input number of pressure layer vertical coordinates from 0.05 to 1100 hPa. The calculations take into account the satellite zenith angle, absorption by well-mixed gases (including nitrogen, oxygen, and carbon dioxide), water vapor (including the water vapor continuum), and ozone.

### 4.1 *Cloud detection algorithm*

MODIS MOD07 atmospheric and surface parameter retrievals require clear sky measurements. The operational MODIS MOD35 cloud mask algorithm (Ackerman et al. 1998) is used to identify pixels that are cloud free. The MODIS cloud mask algorithm determines if a given pixel is clear by combining the results of several spectral threshold tests. A confidence level of clear sky for each pixel is estimated based on a comparison between observed radiances and specified thresholds. The operational retrieval algorithm requires that at least 5 of the 25 pixels in a 5x5 field-of-view area be assigned a 95% or greater confidence of clear by the cloud mask. The retrieval for each 5x5 field-of-view area is performed using the average radiance of only those pixels that were considered clear. Since the decision to perform a retrieval depends upon the validity of the cloud mask algorithm, cloud contamination may occur if the cloud mask fails to detect a cloud, and the retrieval may not be made if the cloud mask falsely identifies a cloud.

### 4.2 *Radiance bias adjustment*

The forward model-calculated radiances have biases with respect to the MODIS measured radiances. There are several possible causes including calibration errors, spectral response uncertainty, temperature and moisture profile inaccuracies, and forward model error. The statistical regression and the physical retrieval methods uses both measured and calculated radiances and thus require that this bias be minimized. Techniques developed for computing GOES sounder radiance biases with respect to the forward model (Hayden 1988) were employed in the MODIS atmospheric profile algorithm. Bias adjustment for radiative transfer calculation of MODIS spectral band radiances is demonstrated to have a positive impact on the atmospheric product retrievals.

Radiance bias calculations are routinely computed for the Atmospheric Radiation Measurement's ARM Climate Research Facility (ARM/ACRF), Southern Great Plains (SGP) site for clear scenes with MODIS sensor zenith angle less than $35^{o}$. Observed MODIS radiances, averaged from a 5x5 field-of-view area, are compared with those computed by the same

transmittance model used in the algorithm. The calculations of radiances are performed using the prototype-CRTM model, with temperature and moisture profile input from National Center for Environmental Prediction's Global Data Analysis System (NCEP-GDAS) global analysis data. Skin temperature and emissivity estimates are from regression with MODIS radiances. To establish credibility for the regression-derived skin temperature input, actual observed skin temperature from a ground-based downward-looking infrared thermometer (IRT) that measures the radiating temperature of the ground surface was also used, and the biases computed using the regression-based skin temperature differ very little from those computed using the IRT skin temperature.

A comparison of MODIS products at the ARM/ACRF SGP site with and without the bias correction (not shown) confirms an improvement with the bias corrections. The improvements were primarily apparent for moist cases where the bias correction helped to correct a dry bias. Because the MODIS retrieval algorithm is applied globally, the biases computed at the SGP ARM-CART site may not be appropriate for application at other latitudes and for other ecosystem types. Thus, biases have been computed for other regions of the globe; however, they are less well validated. Future versions of the algorithm will include a more advanced global bias scheme that uses a regression based on air-mass predictors (atmospheric layer thickness, surface skin temperature, and TPW) such as that employed on the TIROS Operational Vertical Sounder (TOVS) (Eyre 1992; Harris and Kelly, 2001). The radiance bias corrections applied in the operational MODIS atmospheric retrieval algorithm may also need to be updated regularly to account for adjustments in the instrument calibration and improvements in the forward model. In addition, the bias values may vary seasonally so the bias corrections calculated from four days in June may need to be updated.

### 4.3 *Regression profile training data set*

In the MODIS retrieval algorithm, global profiles of temperature, moisture, and ozone from the SeeBor profile database (Borbas et al. 2005) are used in the calculations. The SeeBor training database consists of 15,704 global profiles of temperature, moisture, and ozone at 101 pressure levels for clear sky conditions. The profiles are taken from the NOAA-88, ECMWF, and TIGR-3 training datasets, plus ozonesondes are included from 8 NOAA Climate Monitoring

and Diagnostics Laboratory (CMDL) sites, and global radiosondes from the NOAA Forecast Systems Laboratory (FSL) radiosonde database. When ozone profiles were not available with the original profile data (such as CMDL radiosondes), ozone profiles were derived from temperature and moisture profiles developed using a regression algorithm developed by Paul vanDelst. The radiative transfer calculation of the MODIS spectral band radiances is performed with the prototype-CRTM transmittance model for each profile from the training data set to provide a temperature-moisture-ozone profile/MODIS radiance pair. Estimates of the MODIS instrument noise is added into the calculated spectral band radiances.

To limit the retrievals to training data with physical relevance to the observed conditions, the SeeBor dataset was partitioned into the four land and three ocean zones based upon the calculated 11μm brightness temperatures (BT11) shown in Table 4 . When each statistical retrieval is performed, it uses only the subset of the training data corresponding to the BT11 ranges with a $3^{o}$K overlap. The land/ocean BT11 groups were chosen to allow for sufficient profiles in each category while keeping regions with similar surface radiative properties together.

**Table 4:** Brightness temperature zones used in training data and regression retrieval.

| | Zone # | 11μm BT range for training (K) | 11μm BT range for retrievals (K) | Number of profiles |
|---|---|---|---|---|
| **Land** | 1 | < 275 | < 272 | 1978 |
| | 2 | 269-290 | 272-287 | 2538 |
| | 3 | 284-299 | 287-296 | 2807 |
| | 4 | 293-353 | 296-350 | 2226 |
| **Ocean** | 1 | < 286.5 | < 283.5 | 2214 |
| | 2 | 280.5-296 | 283.5-293 | 2900 |
| | 3 | 290-353 | 293-350 | 2437 |

### 4.4 Land surface characterization

To calculate the synthetic MODIS radiances, a physically realistic characterization of the surface is required. Land surface emissivity and skin temperature are assigned to each profile as described below. Surface pressure is taken from the NCEP-GDAS analysis, with bilinear interpolation among neighboring pixels. Global skin temperature over land is characterized as a function of surface air temperature, solar zenith angle (3 categories), and azimuth angles (8 categories). To build the relationship, surface skin temperature measurements from the IRT at the ARM SGP site in Oklahoma were used together with surface air temperature measured by radiosonde from the period April 2001 to October 2003. The difference between the IRT measured surface skin temperature and the radiosonde surface air temperature for 124 clear sky cases is shown as a function of solar zenith and azimuth angles in Figure 2. The relationship defined by Fig. 2 was used to assign a skin temperature to all profiles.

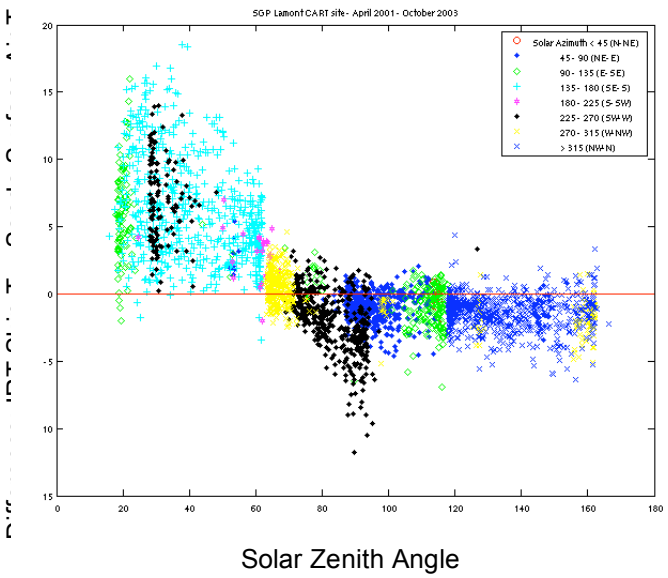


**Figure 2:** Skin Temperature and Surface Air Temperature relationship for the SGP CART site based on clear sky observations between April 2001 and October 2003. Points are colored according to solar azimuth category.

Land surface emissivity values are assigned to the training data profiles based on the Baseline Fit (BF) surface emissivity database. The derivation of the database and its application to the MOD07 retrieval products is described in detail in Seemann et al. (2006) and summarized here. This emissivity is derived using input from the MODIS operational land surface emissivity product (called MOD11). A procedure termed the baseline fit method, based on laboratory measurements (Salisbury and D'Aria, 1992) of surface emissivity, is applied to fill in the spectral gaps between the six MOD11 wavelengths. These MOD11 wavelengths span only three spectral regions: 3.8-4μm, 8.6μm, and 11-12μm, yet the MOD07 retrievals require surface emissivity at higher spectral resolution. BF emissivity is available at 0.05 degree spatial resolution globally at ten wavelengths: 3.7, 5.0, 5.8, 7.6, 8.3, 9.3, 10.8, 12.1, and 14.3 μm. The ten wavelengths were chosen as inflection points to capture as much of the shape of the higher resolution emissivity spectra as possible between 3.6 and 14.3 μm, so emissivity values in between the inflection points can be found by interpolation.

Figure 3 presents a comparison of the TPW in the Sahara desert in northern Africa for Terra ascending (local night) passes on 1 August 2005 between retrievals made with two different

emissivities. When a constant emissivity of 0.95 is used for all bands and profiles, very high TPW values (up to 110mm) with considerable noise are retrieved in this typically dry desert area. This retrieval instability occurs because the regression has not adequately been trained by realistic surface and atmospheric conditions. When the BF emissivity is assigned to the profiles in the training data, the TPW agrees much better with the analysis from the National Centers for Environmental Prediction (NCEP) Global Data Assimilation System (GDAS), also shown in Figure 3. The GDAS analysis includes TPW for both clear and cloudy areas, while MODIS is only a clear-sky algorithm, so GDAS shows higher TPW in the cloudy areas south of the Sahara desert where MODIS has no retrievals.

A closer look at one 5-minute Terra MODIS granule from 2140 UTC of the same day in the north central Sahara desert is shown in Figure 4 for emissivities of 1.0, 0.95, and the BF emissivity. For an emissivity of 1.0, although the TPW magnitudes are more reasonable than for an emissivity of 0.95, there is still along-track striping (noise) and regions of higher TPW than that retrieved with the BF emissivity and that shown by GDAS analysis in Figure 3.

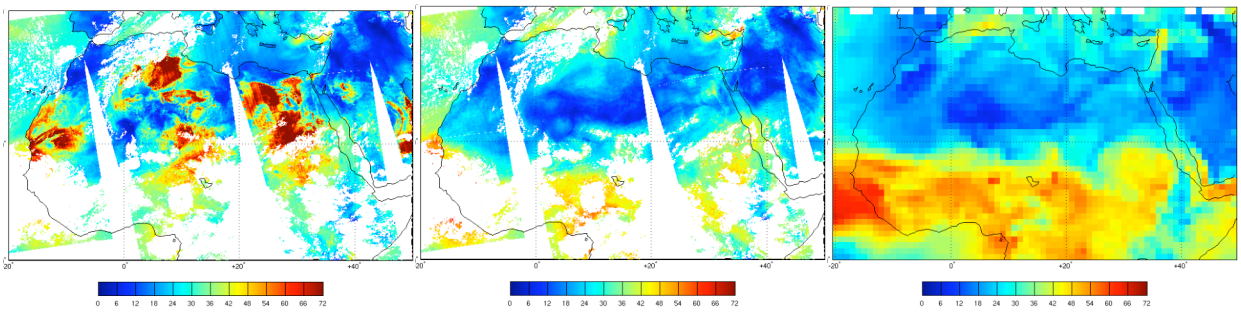

**Figure 3**: TPW retrieved from MOD07 with two different surface emissivities used in the training data (0.95 left, BF center) for all Terra MODIS ascending (nighttime) passes over the Sahara Desert region of Africa on 1 August 2005. MODIS overpass times range from 20:00 UTC (eastern Sahara) to 23:20UTC (western Sahara). For comparison, the 00 UTC NCEP-GDAS TPW analysis from 2 August 2005 is shown (right). The white areas in the MODIS image indicate no retrievals because of either cloudy skies or no MODIS data coverage.

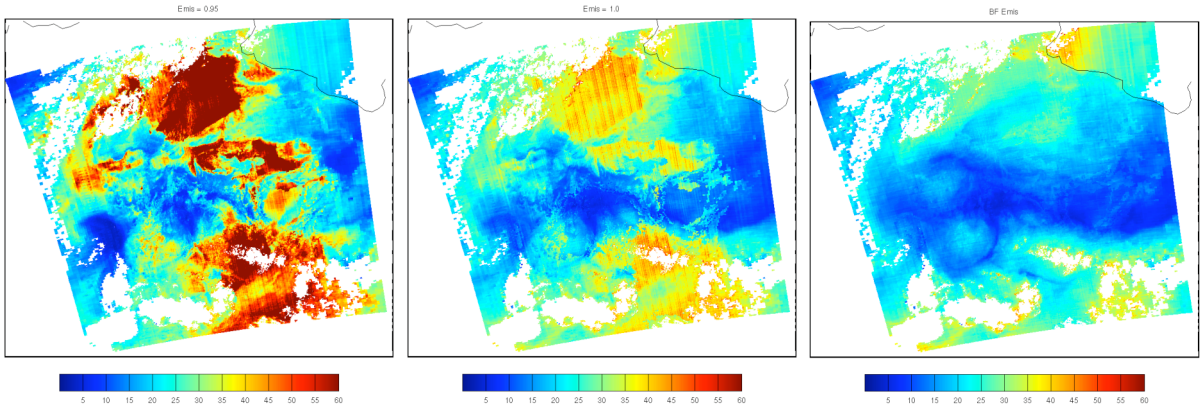


**Figure 4**: MODIS MOD07 TPW for the 5 minute Terra granule beginning at 21:40 UTC on August 1, 2005. This granule is in the north-central Sahara desert and is also shown in Figure 3, although the color scale range is different. Emissivities of 0.95 (left), 1.0 (center), and the baseline fit emissivity (right) were applied to the training data used in the regression retrieval algorithm.

## 5. *Validation of MODIS MOD07 products*

Atmospheric retrievals from MODIS have been compared with those from other observing systems for evaluation of the algorithm. Comparisons are made with measurements from ground-based instrumentation including the ARM SGP site and NOAA/FSL (Forecast Systems Laboratory) GPS sites. Retrievals from other satellites are also used for validation, including the GOES sounder moisture and ozone products, AIRS profiles, and the Special Sensor Microwave/Imager (SSM/I) and Total Ozone Mapping Spectrometer (TOMS). Some of these comparisons are included in this section.

### 5.1 *Comparison of MODIS TPW with ARM SGP observations*

Specialized instrumentation at the ARM/ACRM SGP site in Oklahoma facilitates comparisons of MODIS atmospheric products with other observations collocated in time and space. The Terra satellite passes over the SGP site daily between 0415-0515 UTC and 1700-1800 UTC. Radiosondes are launched three times each day at approximately 0530, 1730, and 2330 UTC. Observations of total column moisture are made by the microwave water radiometer

(MWR) every 40-60 seconds. An additional comparison is possible with the GOES-8 sounder (Menzel and Purdom 1994; Menzel et al. 1998) that retrieves TPW hourly.

Based on manual inspection of radiance images to screen for cloudy cases, a database of clear sky cases at the ARM SGP-ACRF site has been developed for evaluation of the MOD07 total precipitable water (TPW) product. This database includes all overpasses determined to be clear during the period from launch through August 2005: 314 Terra and 302 Aqua cases. MODIS sensor zenith angle was less than 50$^{o}$ to the Lamont, OK SGP site for all cases. These cases can all be reprocessed in-house easily to test any changes to the algorithm or training data. MOD07 TPW is compared with the ARM microwave water radiometer (MWR), radiosonde, and TPW from the GOES satellite for all cases. The comparison for both Terra and Aqua is shown in Figure 5. For Terra, both the original and direct TPW are compared. MOD07 "direct" TPW is retrieved using TPW as a predictor. For the original TPW, moisture profiles are retrieved and integrated. Both variables are saved in the operational MOD07 files.

RMSE for Terra and the MWR is 2.5mm, with an overall bias nearly zero. Aqua shows a higher RMSE, 3.15mm, with an overall bias (MWR-MODIS) of 0.71mm. For only those cases with TPW > 15 mm, the Aqua MODIS TPW is too dry compared with the MWR, with a bias for these 82 cases of 3.41mm. Statistics for both Aqua and Terra compared with the MWR, separated into dry and moist cases are shown in Table 5.

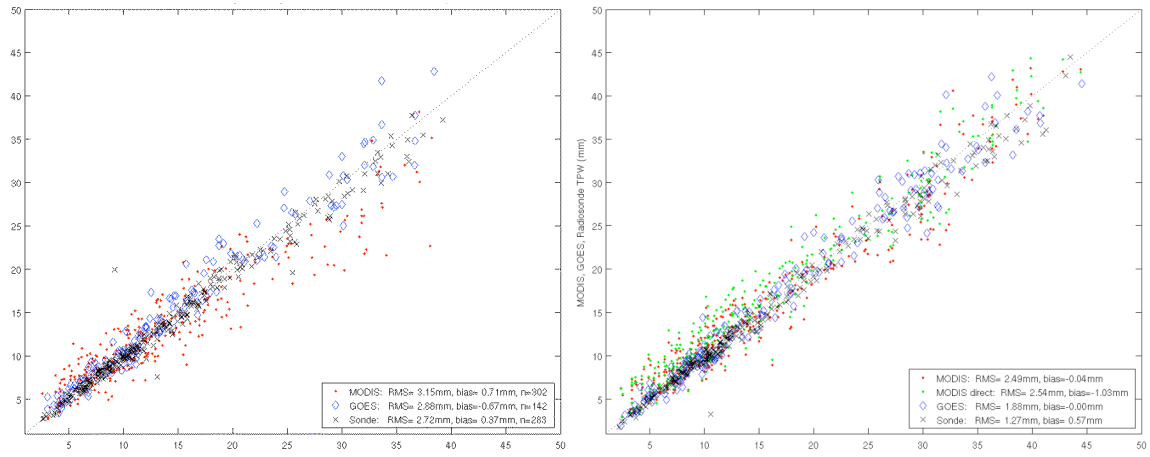


**Figure 5**: Comparison of total precipitable water (mm) at the ARM SGP site from MODIS (y-axis, red dots original, green dots "direct"): Aqua (left) and Terra (right) with the MWR. Also compared with the MWR are GOES-8 and -12 (blue diamonds) and radiosonde (black x's). 302

Aqua and 314 Terra manually-selected clear sky cases from launch through 8/2005 are compared using the MODIS MOD07 algorithm version 5.2.

**Table 5**: RMSE, bias, and number of cases for a comparison between the MWR TPW measured at the ARM SGP site and that from Terra and Aqua MODIS MOD07, GOES, and radiosondes for clear sky cases between April 2001 and August 2005

| | RMSE (mm) | Average Bias (MWR-other) (mm) | N |
|---|---|---|---|
| MOD07, Terra all cases | 2.5 | -0.04 | 314 |
| Terra dry cases (TPW > 15mm) | 2.0 | -0.7 | 202 |
| Terra wet cases (TPW > 15mm) | 3.2 | 1.1 | 112 |
| MOD07, Aqua all cases | 3.2 | 0.7 | 302 |
| Aqua dry cases (TPW > 15mm) | 2.2 | -0.3 | 220 |
| Aqua wet cases (TPW > 15mm) | 4.9 | 3.4 | 82 |
| GOES | 2.0 | -0.1 | 171 |
| Radiosonde | 1.3 | 0.6 | 282 |

### 5.2 *Profile comparisons with AIRS and "Best Estimate" profiles*

As an instrument with moderate spectral resolution, MODIS is not as well equipped for sounding as GOES or AIRS are. However, MODIS can retrieve profiles with a certain degree of accuracy despite its spectral limitations. An evaluation of MOD07 temperature and moisture profiles retrieved with the new BF emissivity is presented in Figure 6. For this comparison, the NASA v4 operational AIRS product, derived from Aqua AIRS radiances, is used. Collocated AIRS and MODIS profile retrievals are compared with the best-estimate (BE) profiles (Tobin et al., 2006) at the SGP ARM site for 80 clear sky Aqua cases between October 2002 and August 2005. The best estimate profiles of the atmospheric state are an ensemble of temperature and moisture profiles created from two radiosondes launched within two hours of the Aqua satellite overpass times. As expected for a sounding instrument, AIRS compares better to the BE profiles

than MODIS. For temperature, the RMSE for MODIS is consistently about 1°K greater than that for AIRS. For mixing ratio, both MODIS and AIRS show similar RMSE relative to the BE profiles above 900hPa, but closer to the surface, MODIS RMSE continues to increase another 0.5g/kg while AIRS RMSE decreases below 900hPa. For mixing ratio bias, however, MODIS bias relative to the BE profiles is near zero at levels above 850hPa, while AIRS bias is somewhat higher. Again, MODIS shows higher biases than AIRS near the surface.

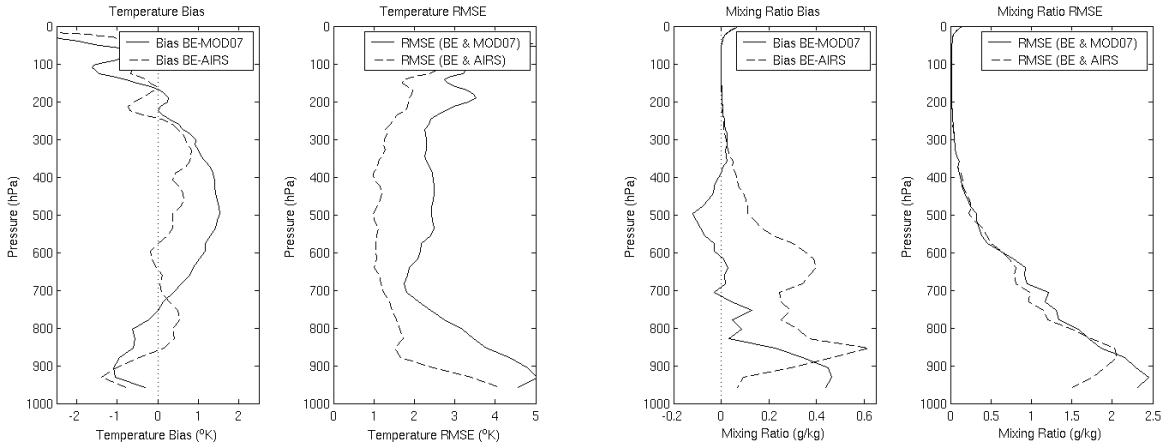


**Figure 6:** Bias and RMS differences between Aqua MODIS MOD07 and AIRS v4 operational temperature and moisture profiles and the "best estimate of the atmosphere" (Tobin et al., 2006) dataset for 80 clear sky cases over the SGP ARM site.

### 5.3 *Comparison of MODIS TPW with GPS site observations*

A near-real time validation processing system has been set up to compare MODIS MOD07 Terra and Aqua TPW with GPS TPW at six U.S. sites. MOD07 data processed from MODIS radiances received by the UW-Madison direct broadcast system of are used and the comparisons are updated automatically twice per day. A map showing the locations of the stations is shown in Figure 7, and results from the first two months of processing are shown in Figures 8 (Terra) and 9 (Aqua), separated by day and night. Near real-time results can be found at the updated MOD07 products page: http://cimss.ssec.wisc.edu/modis/mod07/

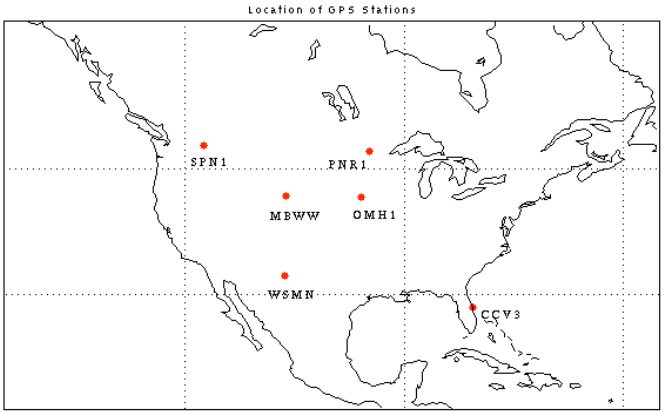


**Figure 7**: Location of GPS sites used for near-real time comparisons with MODIS MOD07 data. Station identifiers are **CCV3:** Cape Canaveral, FL; **PNR1:** Pine River, MN; **WSMN:** White Sands, NM; **OMH1:** Omaha, NE; **SPN1:** Spokane, WA; **MBWW:** Medicine Bow, WY.

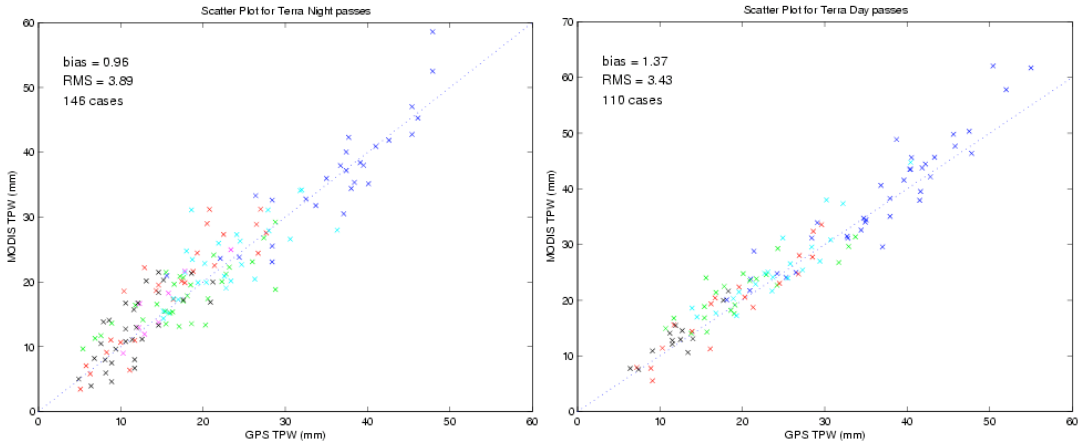


**Figure 8:** Comparison of MODIS MOD07 TPW (mm, y-axis) with GPW TPW (mm, x-axis) for Terra day passes (left panel) and Terra night passes (right panel). Symbols are colored by station, as defined here: CCV3, PNR1, WSMN, OMH1, SPN1, MBWW.

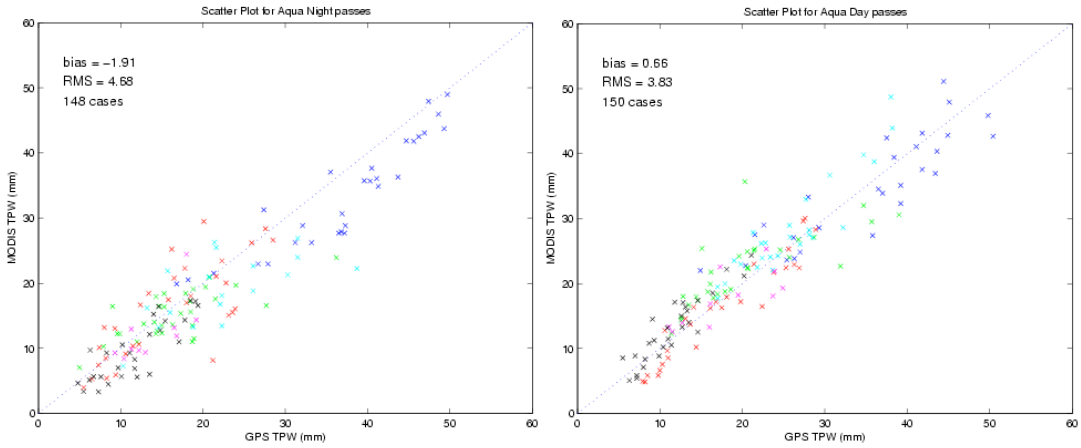


**Figure 9:** As in Figure 8, except for Aqua day (left), and Aqua night (right).

### 5.4 *Comparison with AIRS and MODIS MOD05 Near IR TPW*

Aqua MODIS MOD07 infrared TPW products are also compared with retrievals from Aqua AIRS and MODIS MOD05 near-IR retrievals of water vapor. Figure 10 shows one example of such a comparison for TPW. MODIS MOD07 agrees quite well with the AIRS TPW, particularly over the ocean; however, MODIS MOD05 is somewhat dry in this case. The ability of MODIS to delineate tight gradients in moisture is evident in this comparison. Figure 11 shows a more detailed comparison of one region with a gradient in moisture over the Gulf of Mexico. The high spatial resolution of MODIS allows for more detailed representation of the moisture, however the magnitudes are generally the same. The superior spectral resolution of AIRS enables it to see profiles of temperature and moisture with more detail. This is illustrated in Figure 12, where temperature and moisture profiles from AIRS are compared with those from MODIS.

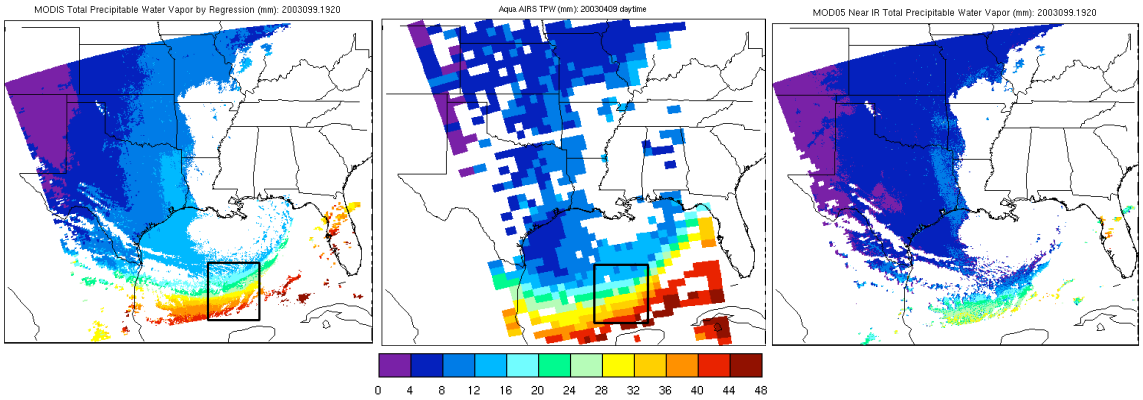


**Figure 10:** Total precipitable water (mm) from Aqua on April 9, 2003. MODIS MOD07 is shown at left, AIRS in the center, and MODIS MOD05 near-IR TPW at right. The region in the Gulf of Mexico within the black box is shown in more detail in Figure 11.

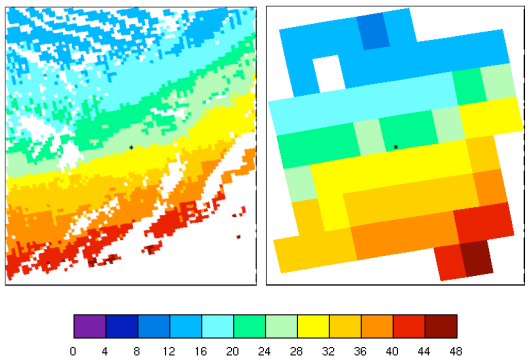


**Figure 11:** TPW (mm) from Aqua MODIS MOD07 (left) and Aqua AIRS (right) for the area within the black boxes in Figure 10. Profiles at the location indicated by the black star are shown in Figure 12.

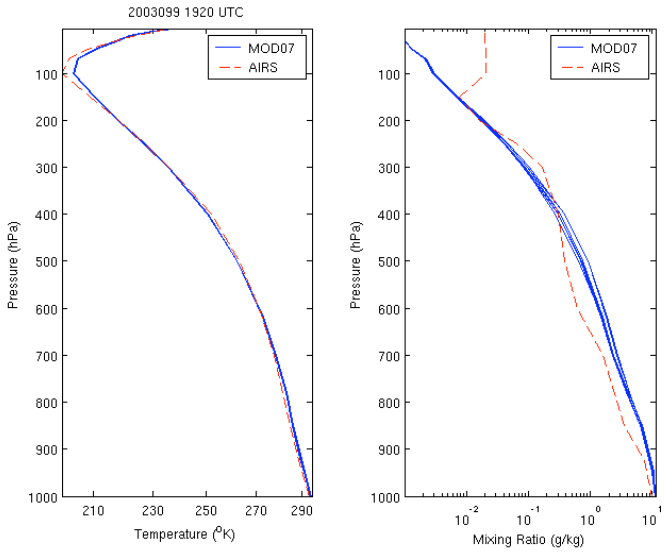


**Figure 12:** Temperature (left) and mixing ratio (right) profiles from Aqua MODIS MOD07 retrievals (blue lines) and Aqua AIRS (red dashed) for the location marked by a black star in Figure 11. Because of the difference in spatial resolution of AIRS and MODIS, 9 MODIS profiles in a 3x3 FOV are shown with the one AIRS profile.

### 5.5 *Continental-Scale comparisons between MODIS and GOES TPW*

On the continental-scale, MODIS TPW was compared to GOES-8 and GOES-10 sounder retrievals of TPW over the continental United States and Mexico. GOES TPW has been well validated (Schmit et al. 2002). GOES has a resolution at the sub-satellite point of 10km and uses radiances measured from a 3 by 3 field of view area (approximately 30 km resolution) to retrieve one atmospheric profile, while MODIS has nadir resolution of 1km and uses a 5 by 5 field of view area (5 km resolution). Unlike the MODIS retrieval, GOES hourly radiance measurements are supplemented with hourly surface temperature and moisture observations as additional information in the GOES retrieval. MODIS and GOES retrieval procedures also use different first guess profiles; GOES uses a numerical model forecast, while MODIS uses the previously described regression retrieval.

Figure 13 compares MODIS TPW to TPW retrieved by the GOES-8 and GOES-10 sounders over North America for 02 June 2001 during the day and at night. The two show fairly good agreement except the MODIS TPW retrieved by regression is drier than GOES over Oklahoma,

Arkansas, and the Gulf of Mexico. TPW retrieved by physical retrieval shows better agreement with GOES in these areas.

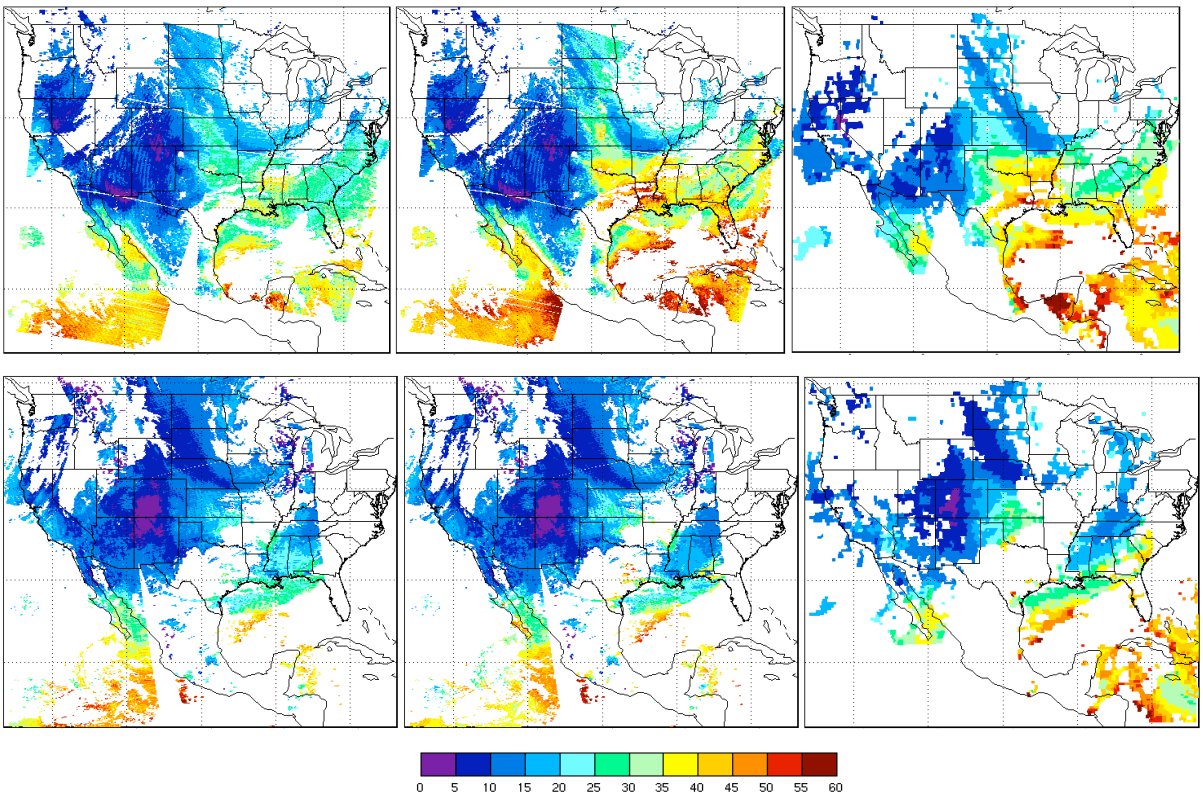


**Figure 13:** Total precipitable water (mm) for 02 June 2001 over North America retrieved by MODIS regression (left), MODIS physical (center), and GOES-8 and GOES-10 (combined, right). The top column shows daytime retrievals (4 MODIS granules from 1640, 1645, 1820, 1825 UTC; GOES at 1800UTC), and the bottom column nighttime (MODIS 0435, 0440, 0445, 0615, 0620 UTC; GOES 06 UTC).

## 5.6 TOMS ozone

The MOD07 total ozone product is routinely compared with the Total Ozone Mapping Spectrometer (TOMS; McPeters et al. 1998, 1996; Bowman and Krueger, 1985) ozone on the global scale for different seasons. One example is shown in Figure 14, a summer case (August 1, 2005) showing elevated ozone in the northern hemisphere and lower in the southern hemisphere. General features in the TOMS ozone are also captured by the MODIS ozone, including the

circular region in the northern Atlantic ocean where ozone is regionally reduced. In the far northern latitudes, however, MODIS ozone is not as high as TOMS is.

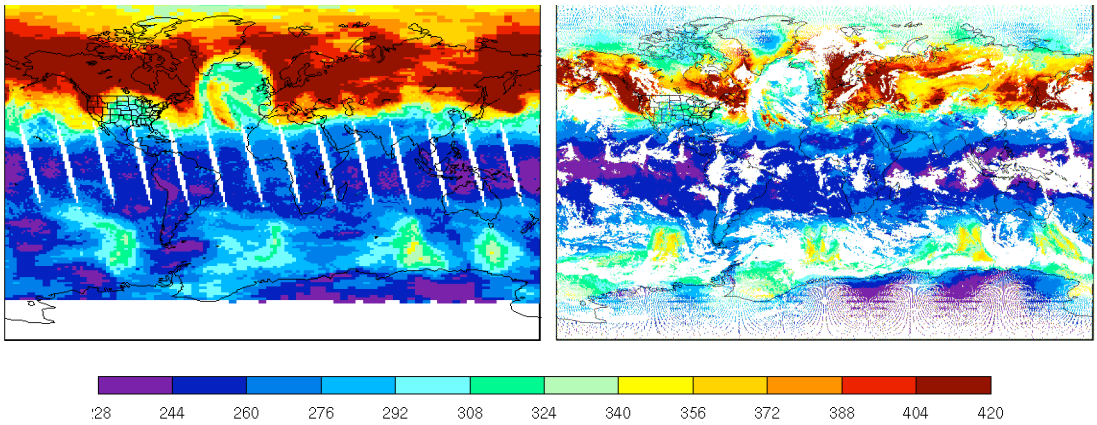


**Figure 14:** Global comparison of Terra MOD07 v5.2 Total Ozone (right, dob) with TOMS/EPT (left) for a summer case August 1, 2005. All MODIS day & night passes were averaged in this comparison. White areas in the MODIS image indicate clouds were present so no retrievals were performed.

## 6.0 *Technical Issues*

The MODIS temperature and moisture profile retrieval algorithm is dependent on the quality of the MODIS Level-1B data provided as input. While instrument noise is important, other factors that affect the quality of retrievals are noisy and/or dead detectors; detector imbalances; mirror side characterization; response vs. scan angle, and spectral shifts. Many of these effects are difficult to characterize and correct, and such corrections are beyond the scope of the temperature and moisture profile retrieval algorithm.

### 6.1 *Destriping of Input MODIS Radiances*

To address across track striping present in the MOD07 retrievals as a result of detector-to-detector differences in radiances, input MODIS L1B 1KM radiances are destriped prior to performing retrievals operationally. The MODIS destriping algorithm is based on the method of

Weinreb et al. (1989). The algorithm accounts for both detector-to-detector and mirror side striping. MODIS is treated as a 20 detector instrument in the emissive bands (10 detectors on each mirror side). The empirical distribution function (EDF) is computed for each detector (cumulative histogram of relative frequency). The EDF for each detector is adjusted to match the EDF of a reference in-family detector. The algorithm operates on L1B scaled integers (0-32767). The median scaled integer value is restored following destriping. Correction LUT is created for each individual granule. Uncorrected scaled integers are replaced with corrected scaled integers (could store the correction LUT instead). Bands 20, 22-25, 27-30, 33-36 are destriped. Impact on bands 31 and 32 is equivocal.

For Terra MODIS, noisy detectors in some bands are replaced with neighbors: 27 (dets 0, 6); 28 (dets 0, 1); 33 (det 1); 34 (dets 6, 7, 8) . For Aqua MODIS, one detector in band 27 is replaced.

### 6.2 *Instrument Errors*

A complete error analysis including the effects of instrument calibration and noise as well as ancillary input data errors remains to be completed. The past performance of these algorithms with HIRS data is documented as temperature profiles errors at about 1.9 C, dewpoint temperature profile errors at about 4 C, total column ozone at about 10%, total column water vapor at about 10%, and gradients in atmospheric stability within 0.5 C. The profile and total atmospheric column algorithms are based on HIRS experience. One significant difference between MODIS and HIRS is the absence of any stratospheric channels on MODIS (15.0, 14.7, and 14.5 μm). This primarily affects the accuracy of the total ozone concentration estimates. The assumption for the MODIS algorithms presented here is that the slowly varying stratospheric temperatures are estimated very well by the forecast model.

### 6.3 *Data Processing Considerations*

Processing is accomplished globally at 5×5 pixel resolution in regions where a sufficient number of clear FOVs are available. Radiances within the clear FOVs are averaged to reduce instrument single sample noise. The algorithm checks the validity of all input radiances, and if

the required input radiance data are bad, suspect, or not available, then the algorithm will record the output products as missing for that 5×5 pixel area. The MODIS Cloud Mask is used for cloud screening and for surface type determination (land or sea). The NCEP GDAS1 6-hourly global analysis estimates of surface pressure at 1 degree resolution are the only non-MODIS ancillary input required for the algorithm.

### 6.4 *Quality Control*

Automatic tests in the code check for physically realistic output values of temperature and moisture. In addition, daily, 8-day, and monthly composites of primary output products such as temperatures at 300, 500, and 700 mb; total precipitable water vapor, and total ozone are routinely monitored for consistency via the MODIS Atmosphere Group website at http://modisatmos.gsfc.nasa.gov/

### 6.5 *Output Product Description*

A single output file (MOD07) combining four products will be generated as part of the MODIS atmospheric profile retrieval algorithm; Table 6 lists the parameters and their units.

**Table 6:** Parameters included in products MOD30, MOD07, MOD38, MOD08
Resolution: 5 × 5 pixel, Temporal sampling: Day and Night, Restrictions: Clear Sky only

| | |
|---|---|
| TAI time at start of scan | (seconds since 1993-1-1 00:00:00.0 0) |
| Geodetic Latitude | (degrees_north) |
| Geodetic Longitude | (degrees_east) |
| Solar Zenith Angle, Cell to Sun | (degrees) |
| Solar Azimuth Angle, Cell to Sun | (degrees) |
| Sensor Zenith Angle, Cell to Sensor | (degrees) |
| Sensor Azimuth Angle, Cell to Sensor | (degrees) |
| Brightness Temperature, IR Bands | (K) |
| Cloud Mask, First Byte | (no units) |

| | |
|---|---|
| Surface Skin Temperature | (K) |
| Surface Pressure | (hPa) |
| Processing Flag | (no units) |
| Tropopause Height | (hPa) |
| Guess Temperature Profile | (K) |
| Guess Dew Point Temperature Profile | (K) |
| Retrieved Temperature Profile | (K) |
| Retrieved Dew Point Temperature Profile | (K) |
| Total Ozone Burden | (Dobsons) |
| Total Totals Index | (K) |
| Lifted Index | (K) |
| K Index | (K) |
| Total Column Precipitable Water Vapor, IR | (cm) |
| Precipitable Water Vapor Low, IR | (cm) |
| Precipitable Water Vapor High, IR | (cm) |

Retrieval Profile Pressure Levels (hPa)
5, 10, 20, 30, 50, 70, 100, 150, 200, 250, 300, 400, 500, 620, 700, 780, 850, 920, 950, 1000

## 7.0 *Future work*

Future work planned for the MOD07 algorithm is listed below:

1. Investigate the dry bias in Aqua TPW and make adjustments to improve.

2. Perform a more thorough evaluation of the ozone product through intercomparisons with TOMS and AIRS and make adjustments to algorithm.

3. Evaluate the current radiance bias adjustments and make updates.

4. Add ozone profiles as output saved to files instead of just total ozone.

5. Assess the TPW Low and TPW High products and possibly change the levels of integration to make them more useful.

6. Improve QA/QC flags and screening for bad input MOD02L1B data.

7. Examine the MOD07 L3 products for consistency with other long term datasets (NVAP).

8. Perform an experimental combined retrieval with AIRS.

9. Update codes to make Aqua and Terra DAAC algorithms uniform.

10. Save MOD07 retrieved infrared land surface emissivity retrievals to operational output files. Currently emissivity is retrieved but only saved for one wavelength.

## 8. *References*

Ackerman, S. A., K. I. Strabala, W. P. Menzel, R. A. Frey, C. C. Moeller, and L. E. Gumley, 1998: Discriminating clear sky from clouds with MODIS. *J. Geophys. Res.,* 103, D24, 32141-32157.

Borbas, E., S. W. Seemann, H.-L. Huang, J. Li, and W. P. Menzel, 2005: Global profile training database for satellite regression retrievals with estimates of skin temperature and emissivity. *Proc. of the Int. ATOVS Study Conference-XIV*, Beijing, China, 25-31 May 2005, pp763-770.

Bowman, K.P. and A.J. Krueger, 1985: A global climatology of total ozone from the Nimbus-7 Total Ozone Mapping Spectrometer", J. Geophys. Res., 90, 7967-7976.

Eyre, J. R., and H. M. Woolf, 1992: A bias correction scheme for simulated TOVS brightness temperatures. *ECMWF Technical Memorandum 186*. 28 pp.

Fleming, H. E. and W. L. Smith, 1971: Inversion techniques for remote sensing of atmospheric temperature profiles. *Reprint from Fifth Symposium on Temperature*. Instrument Society of America, 400 Stanwix Street, Pittsburgh, Pennsylvania, 2239-2250.

Fritz, S., D. Q. Wark, H. E. Fleming, W. L. Smith, H. Jacobowitz, D. T. Hilleary, and J. C. Alishouse, 1972: Temperature sounding from satellites. *NOAA Technical Report NESS 59*. U.S. Department of Commerce, National Oceanic and Atmospheric Administration, National Environmental Satellite Service, Washington, D.C., 49 pp.

Harris, B. A., and G. Kelly, 2001: A satellite radiance bias correction scheme for radiance assimilation. *Quart. J. Roy. Meteor. Soc*., 127, 1453-1468.

Hayden, C. M., 1988: GOES-VAS simultaneous temperature-moisture retrieval algorithm. *J. Appl. Meteor*., **27**, 705-733.

Houghton, J. T., Taylor, F. W., and C. D. Rodgers, 1984: Remote Sounding of Atmospheres. Cambridge University Press, Cambridge UK, 343 pp.

Huang, H.-L. et al., 2004: International MODIS and AIRS Processing Package (IMAPP): A direct broadcast software package for the NASA Earth Observing System. *Bull. Of the American Met. Soc*., 85, No.2, 159-161.

Kaplan, L. D., 1959: Inference of atmospheric structure from remote radiation measurements. *Journal of the Optical Society of America*, **49**, 1004.

King, J. I. F., 1956: The radiative heat transfer of planet earth. *Scientific Use of Earth Satellites*, University of Michigan Press, Ann Arbor, Michigan, 133-136.

King, M.D., Kaufman, Y. J., Menzel, W. P. and D. Tanré, 1992: Remote sensing of cloud, aerosol, and water vapor properties from the Moderate Resolution Imaging Spectrometer

Kleespies, T. J., P. van Delst, L. M. McMillin, and J. Derber, 2004: Atmospheric Transmittance of an Absorbing Gas. 6. OPTRAN Status Report and Introduction to the NESDIS/NCEP Community Radiative Transfer Model. *Appl. Opt*., **43**, 3103-3109.

Li, J., and H.-L. Huang, 1999: Retrieval of atmospheric profiles from satellite sounder measurements by use of the discrepancy principle, *Appl. Optics*, Vol. 38, No. 6, 916-923.

Li, J., W. Wolf, W. P. Menzel, W. Zhang, H.-L. Huang, and T. H. Achtor, 2000: Global soundings of the atmosphere from ATOVS measurements: The algorithm and validation, *J. Appl. Meteorol.,* 39: 1248 – 1268.

Ma, X. L., Schmit, T. J. and W. L. Smith, 1999: A non-linear physical retrieval algorithm – its application to the GOES-8/9 sounder. Accepted by *J. Appl. Meteor*.

McPeters, R.D, Krueger, A.J., Bhartia, P.K., Herman, J.R. et al, 1996: Nimbus-7 Total Ozone Mapping Spectrometer (TOMS) Data ProductsUser's Guide, NASA Reference Publication 1384, available from NASA Center for AeroSpace Information, 800 Elkridge Landing Rd, Linthicum Heights, MD 21090, USA; (301) 621-0390.

McPeters, R.D, Krueger, A.J., Bhartia, P.K., Herman, J.R. et al, 1998: Earth Probe Total Ozone Mapping Spectrometer (TOMS) Data ProductsUser's Guide, NASA Reference Publication 1998-206895 , available from NASA Center for AeroSpace Information, 800 Elkridge Landing Rd, Linthicum Heights, MD 21090, USA; (301) 621-0390.

Menzel, W. P., and J. F. W. Purdom, 1994: Introducing GOES-I: The first of a new generation of geostationary operational environmental satellites. *Bull. Amer. Meteor. Soc.*, **75**, 757-781.

Menzel, W. P., F. C. Holt, T. J. Schmit, R. M. Aune, A. J. Schreiner, G. S. Wade, and D. G. Gray, 1998. Application of the GOES-8/9 soundings to weather forecasting and nowcasting. *Bull. Amer. Meteor. Soc*., **79**, 2059-2077.

Rodgers, C. D., 1976: Retrieval of atmospheric temperature and composition from remote measurements of thermal radiation. *Rev. Geophys. Space Phys.*, **14**, 609-624.

Salisbury, J.W., and D.M. D'Aria, 1992: Emissivity of terrestrial materials in the 8-14mm atmospheric window. *Remote Sensing of the Environment*, **42**, 83-106.

Schmit, T. J., Feltz, W. F., Menzel, W. P., Jung, J., Noel, A. P., Heil, J. N., Nelson, J. P., and G.S.Wade, 2002: Validation and Use of GOES Sounder Moisture Information. *Wea. Forecasting,* **17,** 139-154.

Seemann, S. W., J. Li, W. P. Menzel, and L. E. Gumley, 2003. Operational retrieval of atmospheric temperature, moisture, and ozone from MODIS infrared radiances. *J. Appl. Meteor*., **42**, 1072-1091.

____, Borbas, E., Knuteson, R., Weisz, E., Stephenson, G., Li, J., Huang, H-L., 2006: A global infrared surface emissivity database for clear sky sounding retrievals from satellite-based radiance measurements. submitted to *J. Appl. Meteor*., 2006.

Smith, W. L., Woolf, H. M., and W. J. Jacob, 1970: A regression method for obtaining real-time temperature and geopotential height profiles from satellite spectrometer measurements and its application to Nimbus 3 "SIRS" observations. *Mon. Wea. Rev.*., **8**, 582-603.

____, Woolf, H. M., Hayden, C. M., Wark, D. Q. and L. M. McMillin, 1979: The TIROS-N operational vertical sounder. *Bull*. *Amer*. *Meteor*. *Soc*., **60**, 1177-1187.

____, Suomi, V. E., Menzel, W. P., Woolf, H. M., Sromovsky, L. A., Revercomb, H. E., Hayden, C. M., Erickson, D. N. and F. R. Mosher, 1981: First sounding results from VAS-D. *Bull*. *Amer*. *Meteor*. *Soc*., **62**, 232-236.

____, and F. X. Zhou, 1982: Rapid extraction of layer relative humidity, geopotential thickness, and atmospheric stability from satellite sounding radiometer data. *Appl*. *Opt.*, **21**, 924-928.

____, and H. M. Woolf, 1988: A Linear Simultaneous Solution for Temperature and Absorbing Constituent Profiles from Radiance Spectra. Technical Proceedings of the Fourth International TOVS Study Conference held in Igls, Austria 16 to 22 March 1988, W. P. Menzel Ed., 330-347.

____, 1991: Atmospheric soundings from satellites - false expectation or the key to improved weather prediction. *Jour. Roy. Meteor. Soc.*, **117**, 267-297.

____, Woolf, H. M., Nieman, S. J., and T. H. Achtor, 1993: ITPP-5 - The use of AVHRR and TIGR in TOVS Data Processing. Technical Proceedings of the Seventh International TOVS Study Conference held in Igls, Austria 10 to 16 February 1993, J. R. Eyre Ed., 443-453.

Tobin, D. C., H. E. Revercomb, R. O. Knuteson, B. M. Lesht, L. L. Strow, S. E. Hannon, W. F.

Feltz, L. A. Moy, E. J. Fetzer, and T. S. Cress 2006: Atmospheric Radiation Measurement site atmospheric state best estimates for Atmospheric Infrared Sounder temperature and water vapor retrieval validation, J. Geophys. Res., 111, D09S14, doi:10.1029/2005JD006103.

Twomey, S., 1977: An introduction to the mathematics of inversion in remote sensing and indirect measurements. Elsevier, New York.

Wark, D. Q., 1961: On indirect temperature soundings of the stratosphere from satellites. *J. Geophys*. *Res*., **66**, 77.

____, Hilleary, D.T., Anderson, S. P., and J. C. Fisher, 1970: Nimbus satellite infrared spectrometer experiments. *IEEE. Trans. Geosci. Electron*., **GE-8**, 264-270.

Weinreb et al., 1989: Destriping GOES Images by Matching Empirical Distribution Functions. Remote Sens. Environ., 29, 185-195.